An ab Initio Study on [1,2] Rearrangement Reactions of Silylmethanol H_3SiCH_2OH

Yongming Yu[†,‡] **and Shengyu Feng***[,†]

School of Chemistry and Chemical Engineering, Shandong University, Jinan 250100, P.R. China, and School of Chemistry and Chemical Engineering, Qingdao University, Qingdao 266071, P.R. China

Received: April 25, 2004; In Final Form: June 25, 2004

The [1,2] rearrangement reactions of silylmethanol H_3SiCH_2OH were studied by ab initio calculations at the G2(MP2) levels. The reaction mechanisms were revealed through ab initio molecular orbital theory. The structures of reactants, transition states, and products were located and fully optimized at the MP2(full)/6-31G(d) levels, and the G2(MP2) energies were obtained. On the basis of the MP2(full)/6-31G(d) optimized geometries, harmonic vibrational frequencies of various stationary points were calculated. The reaction paths were investigated and confirmed by intrinsic reaction coordinate calculations. The results show that the [1,2] rearrangements of silylmethanol H_3SiCH_2OH happen in two ways. One is via the Brook rearrangement reactions (reaction A), and the silyl group migrates from carbon atom to oxygen atom passing through a double three-membered ring transition state, forming methoxysilane. The other is that the hydroxyl group migrates from carbon atom to silicon atom, forming methylsilanol (reaction B). The barriers for the reactions A and B were computed to be 348.2 and 240.9 kJ/mol at the G2(MP2) levels, respectively. Changes (ΔS, ΔH, and ΔG) in thermodynamic functions, equilibrium constant $K(T)$, and preexponential factor $A(T)$ and reaction rate constant $k(T)$ in Eyring transition state theory were calculated over a temperature range of 300−1300 K, and then thermodynamic and kinetic properties of the reactions were analyzed.

1. Introduction

Carbofunctional organosilicon compounds play important roles in organosilicon chemistry. For example, they could be used to synthesize new organosilicon compounds or polymers or to modify organosilicon or organic polymers.[1] However, because of the rearrangement or decomposition under certain conditions, their applications are limited to some extent. Understanding their rearrangement conditions and mechanisms will be of great important values for the control and application of these reactions and compounds.

The [1,2] rearrangement reactions of silyl group in α-silyl alcohols from carbon to oxygen atoms[2−10] and in alkyloxysilanes from oxygen to carbon atoms[11−13] under either strong base[2,3,11,12] or peroxide-initiating conditions[4−10,13] are known as Brook and Wright−West rearrangements, respectively (Scheme 1). Studies on the mechanisms of these reactions were focused both experimentally[2,3,8−10,13] and theoretically.[14−17] The ab initio investigations of rearrangement reactions of $[H_2COSiH_3]^-$ and $[H_2COSiH_3]Na$ by Tonachini[14,15] and Wang[16] suggest that the Brook or Wright−West rearrangement under strong base condition occurs via a three-membered ring intermediate (Scheme 2a) in which silicon is pentacoordinate, whereas Schiesser[17] suggested that the rearrangement of $[H_3SiCH_2O]^•$ initiated by peroxide proceed via a three-membered ring transition state (Scheme 2b) in which silicon is also pentacoordinate. Up to now, however, no reports on thermal Brook or Wright−West rearrangement have been found. But actually, there are many occasions that hydroxyalkyl organosilicon compounds or polymers are used under high-temperature conditions. Therefore, understanding their thermal stability or rearrangements is of practical value. In this paper, studies of the thermal rearrangement reactions of silylmethanol H_3SiCH_2OH at the G2(MP2)[18] levels and the analysis of its thermodynamic and kinetic properties using Eyring transition state theory and statistical mechanical methods[19] will be reported.

SCHEME 1

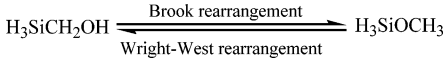

SCHEME 2

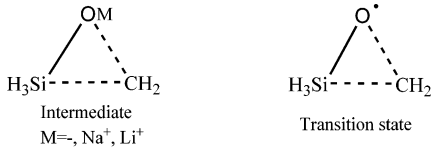

2. Theoretical Methods

Optimized geometries for the stationary points were located at the MP2(full)/6-31G(d) levels. The corresponding harmonic vibrational frequencies (scaled by 0.9427)[20] were calculated at the MP2(full)/6-31G(d) levels in order to verify whether the stationary points are local minimums or first-order saddle points. Energies of stationary points were obtained at the G2(MP2) levels. The reaction paths were examined by intrinsic reaction coordinate (IRC) calculations at the MP2(full)/6-31G(d) levels. The Gaussian 98 series of programs[21] were employed in all calculations. The changes of thermodynamic functions, entropy (ΔS), entropy ($DS^{\neq}$) for transition state, enthalpy (ΔH) and free energy (ΔG), and equilibrium constant ($K(T)$) of reactions were calculated by using the MP2(full)/6-31G(d) optimized geom-

* To whom correspondence should be addressed. Fax: 86-531-8564464. E-mail: fsy@sdu.edu.cn.
† Shandong University.
‡ Qingdao University.

10.1021/jp048197v CCC: $27.50
Published on Web 08/18/2004

SCHEME 3

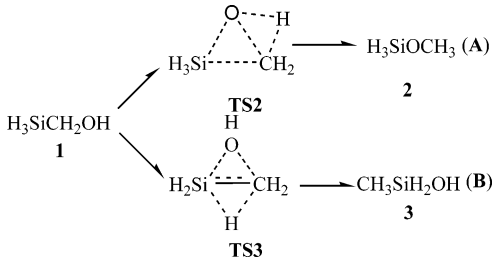

etries and harmonic vibrational frequencies of reactants and products with statistical mechanical methods.[19] Using Eyring transition state theory, the preexponential factor $A(T)$ and rate constant ($k(T)$) of the reactions were obtained.

3. Results and Discussion

The [1,2] rearrangements of silylmethanol **1** could happen in two ways (see Scheme 3). One is that **1** undergoes the Brook rearrangement reactions and the silyl group of **1** migrates from carbon atom to oxygen atom, passing through the double three-membered ring transition state **TS2**, as shown in Scheme 3, path A, forming methoxysilane **2**; the other is that the hydroxyl group of **1** migrates from carbon atom to silicon atom via transition state **TS3**, as shown in Scheme 3, path B, forming methylsilanol **3**. The two pathways of the reactions were investigated.

3.1. Stationary Points. Geometries of H_3SiCH_2OH and its rearrangement products and transition states are given in Figure 1, and the corresponding structural parameters and energies (via ZPE corrections) are listed in Tables 1 and 2, respectively.

The calculations show that reactant **1** exists in two stable geometries, **1a** and **1b**, and that geometry **1a** is slightly more stable than **1b** by 2.4 kJ/mol. IRC calculations indicate that **1a** isomerizes to **1b** via transition state **TS1** with a barrier of only 3.6 kJ/mol, being very easy to interisomerize. Geometry 2 is the only minimum of methoxysilane located on the CH_6OSi

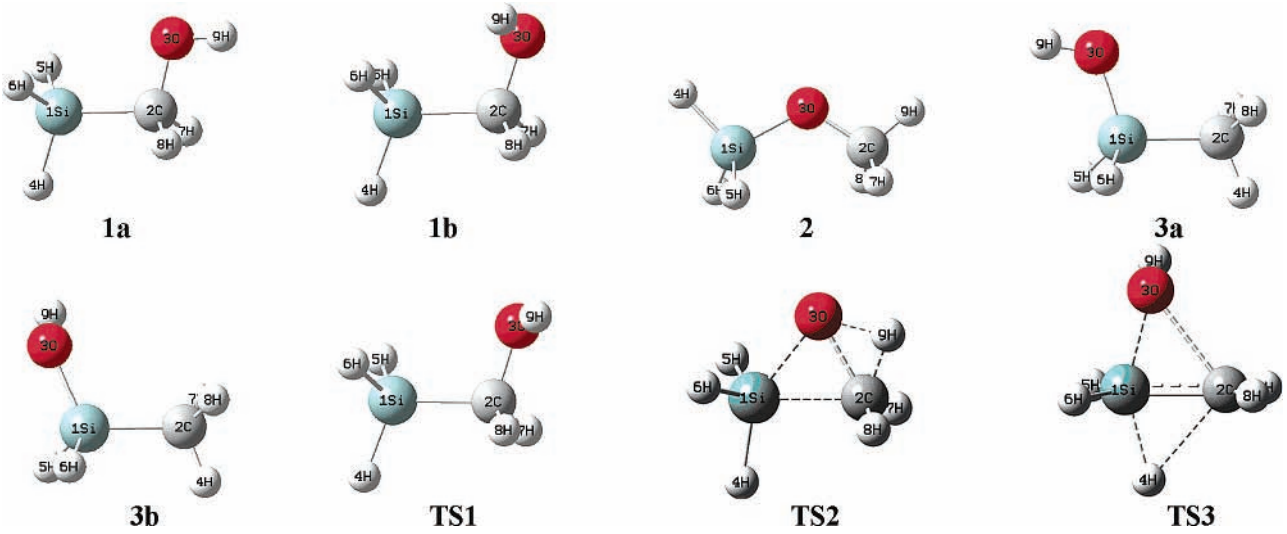

Figure 1. The MP2(full)/6-31G(d) geometries of stationary points.

TABLE 1: The MP2(full)/6-31G(d) Structural Parameters[a]

parameter	1a	TS2	2	1b	TS3	3a	3b	TS1
Si−C	1.893	1.966		1.897	1.800	1.862	1.872	1.894
Si−O		1.874	1.666		1.821	1.674	1.675	
C−O	1.436	1.630	1.426	1.443	2.191			1.447
Si−H^4	1.488	1.512	1.478	1.488	1.642			1.490
Si−H^5	1.483	1.484	1.489	1.483	1.488	1.491	1.491	1.482
Si−H^6	1.483	1.484	1.489	1.488	1.478	1.491	1.481	1.485
C−H^4					2.120	1.094	1.095	
C−H^7	1.099	1.084	1.096	1.093	1.091	1.093	1.094	1.096
C−H^8	1.099	1.084	1.096	1.099	1.090	1.093	1.093	1.097
C−H^9		1.204	1.090					
O−H^9	0.972	1.260		0.972	0.974	0.969	0.969	0.969
SiCO	105.8	62.0	32.6	110.2	53.2	34.5	31.4	106.7
SiOC	43.0	67.9	119.9	40.3	52.3	39.1	35.7	42.3
H^4SiC	109.0	100.7	134.0	111.5	75.7			110.8
H^5SiC	109.9	115.1	96.1	109.9	121.2	110.6	108.5	109.5
H^6SiC	109.9	115.1	96.1	108.0	120.1	110.5		108.9
H^7CSi	110.4	107.6	93.6	110.6	122.9	110.8	112.0	112.2
H^8CSi	110.4	107.6	93.6	112.6	123.5	110.9	110.3	111.2
H^9OC	107.9	47.1	30.6	107.1	114.0			107.9
H^9OSi						116.5	116.3	
H^4SiCO	180.0	180.0	0.0	180.0	178.6	179.7	−177.1	176.5
H^5SiCO	60.5	70.9	−125.6	62.4	92.6	120.1	123.3	56.0
H^6SiCO	−60.3	−70.9	125.6	−56.3	−91.1	−120.8	−116.8	−63.7
H^7CSiO	−120.8	−110.9	125.4	−116.0	−93.9	−59.6	−63.3	−118.8
H^8CSiO	−120.1	110.9	−125.4	124.9	90.5	60.2	57.5	121.9
H^9OCSi	180.0	180.0	180.0	68.5	−104.3	−0.7	−124.2	118.8

[a] Bond lengths are in angstrom; bond and dihedral angles are in degree.

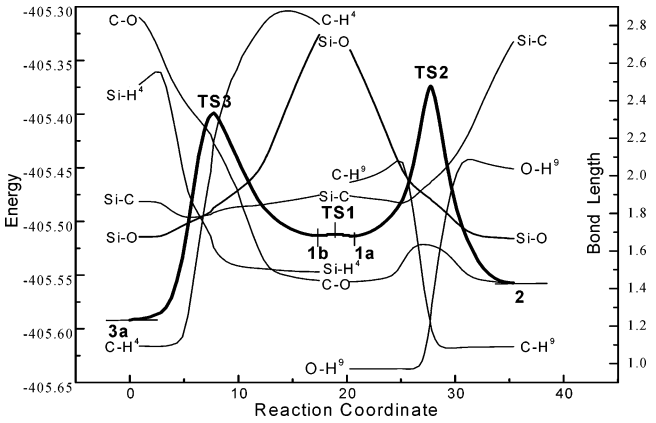

Figure 2. Energy and bond length vs reaction coordinate at the MP2-(full)/6-31G(d) levels.

TABLE 2: Total Energies and Relative Energies of Stationary Points

	MP2(full)/6−31(d)		G2(MP2)	
structure	total energies (a.u.)	rel energies (kJ/mol)	total energies (a.u.)	rel energies (kJ/mol)
1a	−405.449578	0.0	−405.772 970 4	0.0
TS2	−405.315182	352.9	−405.640 352 3	348.2
2	−405.494218	−117.2	−405.811 297 7	−100.7
1b	−405.448952	1.6	−405.772 051 5	2.4
TS3	−405.339214	289.8	−405.680 286 5	243.3
3a	−405.526028	−204.3	−405.848 794	−199.1
3b	−405.525416	−200.7	−405.848 206 4	−197.6
TS1	−405.447985	4.5	−405.771 594 1	3.6

potential energy surface, in which hydrogen atoms on the carbon and silicon are interoverlapped. Other geometries in which hydrogen atoms of carbon and silicon are staggered to each other were proved not to be minimums at MP2(full)/6-31G(d) levels. This is consistent with previous calculations.[22] Minimums **3a** and **3b** are two stable isomeric conformations of methylsilanol **3**. Similar to the situation in reactants **1a** and **1b**, the minimum **3a** is slightly more stable than **3b**. The energy difference between **3a** and **3b** is only 1.5 kJ/mol. First-order saddle points **TS2** and **TS3** were verified by IRC calculations (Figure 2) to be the transition states from **1a** to **2** and **1b** to **3a**, respectively. In **TS2** and **TS3**, silicon atoms are pentacoordinate. The distances of C−O, C−H^9, and O−H^9 bonds in **TS2** are 1.630, 1.260, and 1.204, respectively, a little longer than those in **1a**, **2**, and **1a**, respectively. It indicates that there are weak bonding interactions between C and O, H^9 and C, and H^9 and O. Therefore, **TS2** could be viewed as a bicyclic structure with two three-membered rings. In **TS3**, the atoms in the H^5 H^6Si−CH^7H^8 moiety are nearly coplanar, and the Si−C bond length is between those of Si═C in H_2Si═CH_2 and Si−C in reactant **2**. This suggests that the Si−C bond has partly double bond features.

3.2. The [1,2] Migration of the Silyl Group from Carbon to Oxygen. The IRC calculations (see Figure 2) show that the [1,2] migration of the silyl group (H_3Si−) of H_3SiCH_2OH from the carbon to the oxygen to form methoxysilane happens as a one-step transposition passing through the transition state **TS2**. In the beginning of the reaction, coupled with the motion of H^9 toward the carbon atom, the oxygen atom of reactant **1** moves toward the silicon atom. During the process, the C−O and H^9−O bonds weaken, and the Si−O and H^9−C distances gradually shorten. Before the H^9−O bond fully dissociates, the C−O distance reaches its maximum and then begins to shorten. As a result, the transition state **TS2** was reached. The C−O and H^9−O distances increase from 1.436 and 0.972 in reactant **1** to 1.630 and 1.260 in **TS2**, respectively. Meanwhile, the Si−O and H^9−C distances reduce from 2.670 and 1.966 to 1.874 and 1.204, respectively. The activation barrier for reaction A is 348.2 kJ/mol.

Getting over the transition state, as the oxygen atom further approaches the carbon atom, the carbon atom leaves the silicon atom gradually, coupled with the rotation of the CH_3 group rounding an axis perpendicular to the SiOC plane in the direction of the H^9 apart from the oxygen atom. As a result, product **2** forms as the oxygen atom fully bonds to the carbon atom and the Si−C bond fully dissociates. The IRC calculations also show that during the [1,2] migration of the silyl group, the configuration of the silyl group is sterically retained.

The rearrangement reaction A can also be analyzed from the change of the MP2(full)/6-31G(d) atomic natural charges based on the MP2(full)/6-31G(d) optimized geometries in molecules (see Table 3). As the reaction proceeds, a partial lone pair of electrons of the oxygen atom transfer to the silicon atom, and more valence electrons of the silicon atom transfer to the carbon atom, leading to the corresponding increases of positive charge of the silicon atom and negative charge of the carbon atom and a decrease of the negative charge of the oxygen atom in **TS2**. When **2** forms, the Si−C bond cleaves, and the silicon atom bonds to the oxygen atom, with the result that more valence electrons of the silicon atom transfer to the oxygen atom, with an increase of positive charge of the silicon atom by 0.072 and negative charge of the oxygen atom by 0.203 and a decrease of the negative charge of the carbon atom by 0.659 in **2** in comparison with **TS2**.

3.3. The [1,2] Migration of the Hydroxyl Group from Carbon to Silicon. The IRC calculations indicate that the [1,2] migration (Scheme 3, path B) of the hydroxyl group of H_3SiCH_2OH from the carbon to the silicon to form methylsilanol **3** is a one-step transformation passing through transition state **TS3** in which the silicon is pentacoordinate. The reaction begins as the hydroxyl group of reactant **1b** moves toward the silicon, coupled with the inverse motion of the hydrogen atoms in CH_2. It can be seen from Figure 2 that at the beginning of the reaction, the C−O and Si−H^4 distances lengthen slowly. As the hydroxyl group further approaches the silicon atom, the distances of the C−O and Si−H^4 lengthen rapidly, and the transition state **TS3** is reached. The Si−O distance reduces from 2.750 in **1b** to 1.821 in the **TS3**, and the C−O and Si−H^4 distances increase from

TABLE 3: Atomic Natural Charges

molecule	Si	C	O	H^4	H^5	H^6	H^7	H^8	H^9
1a	1.111	−0.508	−0.803	−0.236	−0.221	−0.221	0.196	0.196	0.485
TS2	1.349	−0.887	−0.778	−0.302	−0.235	−0.235	0.276	0.276	0.535
2	1.421	−0.228	−0.981	−0.248	−0.267	−0.267	0.182	0.182	0.206
1b	1.087	−0.514	−0.793	−0.228	−0.218	−0.234	0.222	0.199	0.480
TS3	1.324	−0.345	−1.125	−0.331	−0.237	−0.220	0.219	0.258	0.487
3a	1.669	−1.199	−1.148	0.240	−0.284	−0.284	0.248	0.248	0.510
3b	1.666	−1.206	−1.145	0.0.244	−0.284	−0.267	0.238	0.246	0.507
TS1	1.104	−0.513	−0.806	−0.236	−0.218	−0.228	0.211	0.198	0.498

TABLE 4: Thermodynamic and Kinetic Analyses

T (K)	$\Delta S^{\neq}$ (J/K)	*k*(*T*) (S^{1-})	ΔH (kJ/mol)	ΔG (kJ/mol)	ΔS (J/K)	*K* (*T*)	*A* (*T*)
			Reaction A				
300	−7.99	0.00×10^{0}	−113.72	−114.21	1.65		6.50×10^{12}
400	−8.49	0.69×10^{-33}	−114.27	−114.30	0.086		8.16×10^{12}
500	−8.85	0.13×10^{-23}	−114.83	−114.24	−1.18		9.77×10^{12}
600	−9.19	0.22×10^{-17}	−115.34	−114.08	−2.11		1.12×10^{13}
700	−9.55	0.59×10^{-13}	−115.78	−113.83	−2.78	3.12×10^{08}	1.26×10^{13}
800	−9.92	0.13×10^{-09}	−116.13	−113.53	−3.26	2.58×10^{07}	1.37×10^{13}
900	−10.29	0.49×10^{-07}	−116.42	−113.18	−3.59	3.71×10^{06}	1.48×10^{13}
1000	−10.66	0.58×10^{-05}	−116.64	−112.81	−3.83	7.81×10^{05}	1.57×10^{13}
1100	−11.03	0.29×10^{-03}	−116.82	−112.42	−4.00	2.18×10^{05}	1.65×10^{13}
1200	−11.40	0.76×10^{-02}	−116.96	−112.01	−4.12	7.51×10^{04}	1.73×10^{13}
1300	−11.76	0.12×10^{00}	−117.06	−111.59	−4.21	3.05×10^{04}	1.79×10^{13}
			Reaction B				
300	−9.28	0.38×10^{-37}	−198.7	−199.9	4.02		5.56×10^{12}
400	−8.64	0.19×10^{-24}	−198.5	−200.4	4.74		8.01×10^{12}
500	−8.06	0.86×10^{-17}	−198.3	−200.9	5.18		1.07×10^{13}
600	−7.73	0.11×10^{-11}	−198.2	−201.4	5.40		1.34×10^{13}
700	−7.62	0.50×10^{-08}	−198.1	−201.9	5.46		1.59×10^{13}
800	−7.68	0.28×10^{-05}	−198.1	−202.5	5.43		1.80×10^{13}
900	−7.87	0.38×10^{-03}	−198.2	−203.0	5.34	5.90×10^{11}	1.98×10^{13}
1000	−8.13	0.19×10^{-01}	−198.3	−203.5	5.23	4.24×10^{10}	2.13×10^{13}
1100	−8.44	0.47×10^{00}	−197.4	−204.1	5.19	4.88×10^{09}	2.26×10^{13}
1200	−8.79	0.68×10^{01}	−198.6	−204.6	5.12	8.03×10^{08}	2.36×10^{13}
1300	−9.15	0.65×10^{02}	−198.7	−205.1	4.89	1.74×10^{08}	2.45×10^{13}

TABLE 5: Vibrational Frequencies[a] (cm^{-1}) and Corresponding Vibrations

vibration	**1a**	**TS2**	**2**	**1b**	**TS3**	**3a**	**3b**	**TS1**
O−H stretching	3550 (25)			3556 (28)	3534 (73)	3614 (81)	3619 (78)	3593 (44)
C−H stretching	2928 (39)	2408 (127)	2976 (38)	2901 (34)				2912 (26)
	2883 (34)		2904 (47)					
Si−H stretching	2202 (162)	2186 (206)	2223 (153)	2199 (136)	2209 (138)	2156 (161)	2208 (163)	2202 (143)
	2195 (111)	2163 (95)	2166 (113)	2174 (182)	2148 (126)	2150 (257)	2152 (205)	2187 (131)
	2170 (131)	2027 (344)	2163 (219)	2166 (94)	1550 (235)			2163 (145)
C−O stretching	1012 (48)		1082 (148)	994 (64)				984 (68)
Si−O stretching						814 (49)	812 (111)	
CH_2 bending					865 (87)			
CH_3 bending		311 (40)	1171 (37)			1299 (39)	1297 (39)	
							751 (64)	
SiH_2 bending						992 (192)	962 (181)	
						718 (70)	935 (241)	
SiH_3bending	931 (45)	1037 (94)	979 (349)	931 (56)	954 (25)			932 (67)
	930 (69)	1036 (233)	947 (165)	930 (55)	937 (140)			930 (46)
	910 (254)	710 (96)	924 (104)	913 (256)	758 (33)			912 (255)
	703 (55)		705 (31)	565 (26)				721 (41)
	575 (31)		699 (68)					573 (27)
others	1159 (33)	901 (376)	745 (58)	1340 (32)	853 (159)	962 (228)	896 (136)	833 (50)
	514 (41)	858 (64)		1111 (45)	643 (45)	877 (61)	870 (41)	
		579 (104)		838 (50)	596 (108)	901 (160)	690 (63)	
		403 (81)			408 (142)	724 (118)		

[a] IR intensity (km/mol) in parentheses.

1.436 and 1.488 to 2.191 and 1.642, respectively. With interaction of the lone pair electrons of the oxygen atom and the empty 3d orbital of the silicon atom in **TS3**, partial valence electrons of the silicon atom transfers to the oxygen atom, resulting in an increase in the positive charge of the silicon atom and the negative charge of the oxygen atom and a a decrease in the negative charge of the carbon atom (see Table 3). The activation barrier for the reaction is 240.9 kJ/mol, lower by 107.3 kJ/mol than rearrangement A.

Getting over the transition structure, the hydroxyl group continuously approaches the silicon atom, and the H^4 departs from the silicon and moves toward the carbon atom. As a result, the hydroxyl group attaches to the silicon atom, coupled with the fully dissociation of $Si-H^4$ bond and the formation of the $C-H^4$ bond, resulting in the formation of product **3a**.

3.4. Thermodynamic and Kinetic Analyses. Thermodynamic and kinetic analyses can further illustrate the realizability and possibility of a reaction, so we carried out the thermodynamic and kinetic calculations for rearrangements A and B. The calculated thermodynamic functions, ΔS, $\Delta S^{\neq}$, ΔH, and ΔG; equilibrium constant $K(T)$; and rate constant $k(T)$ for the reactions over a temperature range from 300 to 1300 K are listed in Table 4. All values are calculated on the basis of the MP2-(full)/6-31G(d) optimized parameters, and energies are corrected by the zero-point energies. It can be found from the data in Table 4 that the ΔH and ΔG values for the two reactions are all negative, indicating that they are exothermic and spontaneous. As the temperature rises, the exothermicity and the ΔG value of reaction A increase. For reaction B, the ΔG value slowly decreases with the rising of temperature from 300 to 1300 K, whereas the exothermicity gradually decreases prior to 700 K and increases after 700 K. In addition, the equilibrium constant $K(T)$ and reaction rate $k(T)$ values of reaction B are larger than those of reaction A at the same temperature. It suggests that

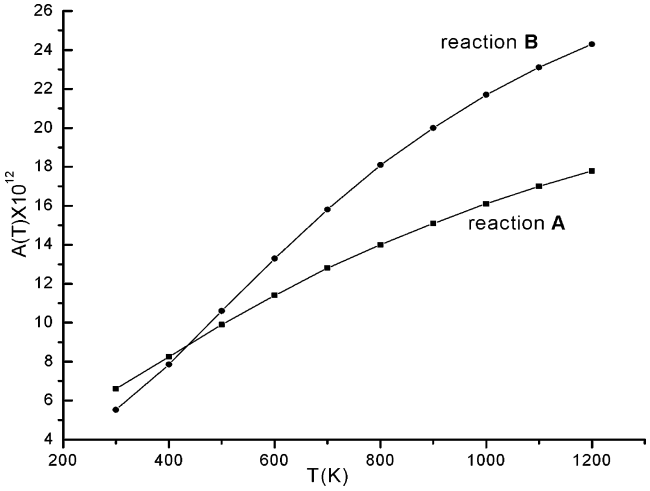

Figure 3. Factor A(T) against temperature (T) for reactions A and B.

the rearrangements of **1** are favorable to route B, both thermodynamically and kinetically. So when **1** is heated, the main rearrangement product would be **3**.

Figure 3 shows the preexponential factor $A(T)$ against temperature (T) for reactions A and B over a temperature range from 300 to 1300 K. It can be found from Figure 3 that reaction B is more sensive to temperature than is reaction A. The relationship between the factor $A(T)$ and temperature T exactly conforms to the following equations:

$$A(T)_{\mathrm{A}} = 7.10 \times 10^{11} + 2.1 \times 10^{10}T - 6.12 \times 10^{6}T^{2}$$

$$A(T)_{\mathrm{B}} = -5.22 \times 10^{12} + 3.84 \times 10^{10}T - 1.19 \times 10^{7}T^{2}$$

So the rate constants for reactions A and B over a temperature range from 300 to 1300 K can be given as follows:

$$k(T)_{\mathrm{A}} = (7.10 \times 10^{11} + 2.1 \times 10^{10}T - 6.12 \times 10^{6}T^{2})\mathrm{e}^{-42.44/T}$$

$$k(T)_{\mathrm{B}} = (-5.22 \times 10^{12} + 3.84 \times 10^{10}T - 1.19 \times 10^{7}T^{2})\mathrm{e}^{-34.65/T}$$

3.5. Vibrational Frequencies. The main vibrational frequencies (scaled by a factor of 0.9427)[20] of reactants, transition states, and products for the two rearrangements are summarized in Table 5. Each frequency is attributed to one or two vibrations, and each molecule has its own characteristic frequencies by which its structures can be confirmed. The data in Table 5 are all consistent with the corresponding molecular structures.

4. Conclusions

The calculations show that two competitive rearrangement reactions may occur when silylmethanol is heated. One is via the Brook rearrangement reaction, and the silyl group migrates from the carbon to the oxygen atom passing through a double three-membered ring transition state, forming methoxysilane. The other is that the hydroxyl group migrates from the carbon to the silicon atom via a double three-membered ring transition state, forming methylsilanol. Silicon atoms in the two transition states are pentacoordinate. The barrier for the Brook rearrangement was computed to be 348.2 kJ/mol at the G2(MP2) levels, 107.3 kJ/mol higher than the hydroxyl group migration reaction (240.9 kJ/mol). Thermodynamic and kinetic analyses indicate that the hydroxyl group migration reaction is preferred to the Brook rearrangement reaction, both thermodynamically and kinetically.

Acknowledgment. This work was supported by the National Natural Science Foundation of China, the Natural Science Foundation of Shandong Province, Reward Funds for the Outstanding Young by Shandong University, Foundation for University Key Teacher by the Ministry of Education, and Scientific Research Starting Fundation for the Return Overseas Chinese Scholar by the Ministry of Education.

References and Notes

(1) Du, Z. D.; Chen, J. H.; Bei, X. L.; Zhou, C. G. *Organosilicon Chemistry*, The High Education Press: Beijing, 1992, pp 175−177.
(2) Brook, A. G. *Acc. Chem. Res.* **1974**, *7*, 77−84.
(3) Reich, H. J.; Holtan, R. C.; Bolm, C. *J. Am. Chem. Soc.* **1990**, *112*, 5609−5617.
(4) Dalton, J. C.; Bourque, R. A. *J. Am. Chem. Soc*. **1981**, *103*, 699−700.
(5) Tsai, Y.-M.; Cherng, C.-D. *Tetrahedron Lett*. **1991**, *32*, 3515−3518.
(6) Chang, S.-Y.; Jiaang, W.-T.; Cherng, C.-D.; Tang, K.; Hang, C.-H.; Tsai, Y.-M. *J. Org. Chem*. **1997**, *62*, 9089−9098.
(7) Robertson, J.; Burrow, J. N. *Tetrahedron Lett*. **1994**, *35*, 3777−3780.
(8) Paredes, M. D.; Alonso, R. *Tetrahedron Lett.* **1999**, *40*, 3973−3976.
(9) Paredes, M. D.; Alonso, R. *J. Org. Chem.* **2000**, *65*, 2292−2304.
(10) Harris, J. M.; MacInnes, I.; Dalton, J. C.; Maillard, B. *J. Organomet. Chem*. **1991**, *403*, C25−C28.
(11) Wright, A.; West, R. *J. Am. Chem. Soc*. **1974**, *96*, 3214−3222.
(12) Linderman, R. J.; Ghannam, A. *J. Am. Chem. Soc.* **1990**, *112*, 2392−2398
(13) Shuto, S.; Kanazaki, M.; Ichikawa, S.; Minakawa, N.; Matsuda, A. *J. Org. Chem.* **1998**, *63*, 746−754.
(14) Antoniotti, P.; Tonachini, G. *J. Org. Chem.* **1993**, *58*, 3622−3632.
(15) Antoniotti, P.; Canepa, C.; Tonachini, G. *J. Org. Chem*. **1994**, *59*, 3952−3959.
(16) Wang, Y.-G.; Dolg, M. *Tetrahedron* **1999**, *55*, 12751−12756.
(17) Schiesser, C. H.; Styles, M. L. *J. Chem. Soc., Perkin Trans. II* **1997**, *2*, 2335−2340.
(18) Curtiss, L. A.; Krishnan, R.; Pople, J. A. *J. Chem. Phys.* **1993**, *98*, 1293.
(19) Ju, G.; Feng, D.; Deng, C. *Acta Chim. Sin.* **1985**, *43*, 680.
(20) Foresman, J. B.; Frisch, A. *Exploring Chemistry with Electronic Structure Methods*, 2nd ed.; Gaussian, Inc.: Pittsburgh, PA, 1996, p64.
(21) Frisch, M. J.; Trucks, G. W.; Schlegel, H. B.; Scuseria, G. E.; Robb, M. A.; Cheeseman; Zakrzewski, V. G.; Montgomery, J. A., Jr.; Stratmann, R. E.; Burant, J. C.; Dapprich, S.; Millam, J. M.; Daniels, A. D.; Kudin, K. N.; Strain, M. C.; Farkas, O.; Tomasi, J.; Barone, V.; Cossi, M.; Cammi, R.; Mennucci, B.; Pomelli, C.; Adamo, C.; Clifford, S.; Ochterski, J.; Petersson, G. A.; Ayala, P. Y.; Cui, Q.; Morokuma, K.; Malick, D. K.; Rabuck, A. D.; Raghavachari, K.; Foresman, J. B.; Cioslowski, J.; Ortiz, J. V.; Baboul, A. G.; Stefanov, B. B.; Liu, G.; Liashenko, A.; Piskorz, P.; Komaromi, I.; Gomperts, R.; Martin, R. L.; Fox, D. J.; Keith, T.; Al-Laham, M. A.; Peng, C. Y.; Nanayakkara, A.; Challacombe, M.; Gill, P. M. W.; Johnson, B.; Chen, W.; Wong, M. W.; Andres, J. L.; Gonzalez, C.; Head-Gordon, M.; Replogle, E. S.; Pople, J. A. *Gaussian 98*, Revision A.9; Gaussian, Inc.: Pittsburgh, PA, 1998.
(22) (a) Ignat'ev, I. S.; Shchegolev, B. F. *Phys. Chem.* (Russian) **1987**, *296* (1), 143−147. (b) Grigoras, S.; Lane, T. H. *J. Comput. Chem*. **1987**, *8*, 84. (c) Oberhammer, H.; Boggs, J. E. *J. Am. Chem. Soc*. **1980**, *102*, 7241. (d) Raghavachari, K.; Chandrasekhar, J.; Frisch, M. J. *J. Am. Chem. Soc*., **1982**, *104*, 3779.